

Development of ultrafiltration membranes from acrylonitrile co-polymers

Heriberto Espinoza-Gómez, Shui Wai Lin (✉)

Centro de Graduados e Investigación del Instituto Tecnológico de Tijuana,
Apdo Postal 1166, Tijuana B.C. México
e-mail: jhespinoza@hotmail.com, Tel.: +(52)662 337 72

Received: 29 April 2001/Revised version: 14 September 2001/Accepted: 14 September 2001

Summary

Hydrophobic polymer surfaces show higher tendency to protein adsorption and bacteria attachment, thus hydrophobic polymeric membranes foul rapidly in water purification operations. A change in membrane surface properties can reduce fouling; this may be accomplished by increasing the hydrophilicity of the membrane surface, and by using a membrane with smaller pore size. The ultrafiltration membranes were prepared via phase inversion process in our laboratory. Negatively charged hydrophilic ultrafiltration membranes were prepared from acrylonitrile-vinyl acetate (CP16)/Acrylonitrile-vinyl acetate-sodium p-sulfophenyl methallyl ether (CP24). Scanning electron microscopy (SEM) revealed the asymmetric structure of these membranes. The roughness of the surface was measured by atomic force microscopy (AFM). The basic characteristics of these membranes like water permeability, water content and membrane selectivity were also measured.

Keywords: Ultrafiltration, PAN-membrane, Hydrophilic Membrane, Membrane Preparation and Structure

Introduction

The demand for membrane separation systems is growing rapidly each year [1-3]. In spite of the success of membrane technology, membrane separation systems suffer from a serious problem: the membrane fouling [4]. Membrane fouling is caused mainly by (a) plugging the pore openings at the porous membrane surface by the suspended solid particles or large solutes in the feed and (b) the attachment of bacteria and subsequently colonization on the membrane surface [5]. For ultrafiltration membranes the biofouling can be minimized by periodical cleaning with sodium hypochlorite, by which the biofilm would be mostly washed away. The membrane system thus regains most of its permeate flow rate. The membrane fouling due to plugging by solid particles or by large solutes is an irreversible process and ordinary cleaning methods do not recover the lost of permeate flow. The passage of water through these obstructed pore-openings is hindered and in order to maintain the permeate flow to a desired level, application of higher filtration pressure is needed.

Generally, proteins are adsorbed more strongly at hydrophobic surfaces than hydrophilic surfaces [6-7]. Initial biofilm formation is achieved by bacteria attachment through exopolymer synthesis at the membrane surface; this would be avoided if the membrane surface were hydrophilic in nature. Most of the hydrophilic UF membranes have fixed negative charges at the membrane surface; this negative surface charges prevent the

negatively charged colloidal particles to settle on the membrane surface, and therefore it slows down the membrane fouling process [7]. In this study we had focused on how to improve membrane-fouling resistance by increasing the negative surface density of the membrane and by increasing the hydrophilicity of the neutral membrane.

The performance of an asymmetric polymeric membrane must be closely related to the morphology of the dense layer [8-10], where separation properties against solutes (the so-called cut-off) arise [11-13]

In this work we investigated negatively charged hydrophilic membranes from PAN copolymers (CP16/CP24). In all of our membrane preparations we used NMP as a solvent. Figure 1 shows the chemical structures of the CP16 and CP24 polymers. Our membranes were made by a phase inversion process.

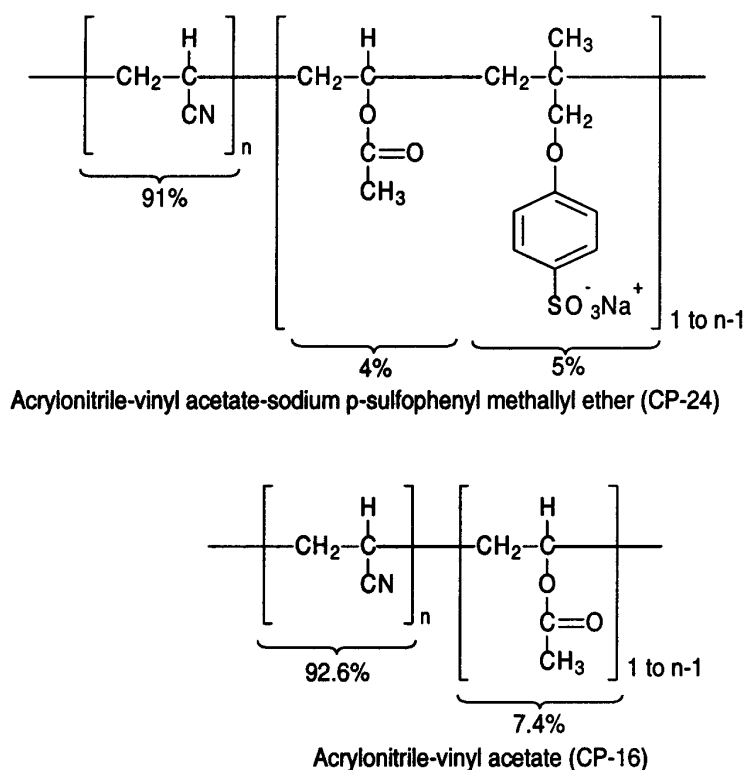


Figure 1 Chemical Structures of CP24 (charged) and CP16 (neutral) polymers.

Experimental

Materials

Dextran T-70 (70,000 Daltons) and Dextran T-500 (500,000 Daltons) - Pharmacia.

Dextrans of Average Molecular Weights of 162,000 and 298,000 Dalton - Sigma.

1-Methyl-2-pyrrolidinone (NMP) - Aldrich Chemical Company, Inc.

Acrylonitrile-vinyl acetate (CP-16) - Solutia

Acrylonitrile-vinyl acetate p-sulfophenyl methallyl ether (CP-24) - Solutia

Instruments

Burleigh II Atomic Force Microscope

JSM5300 Scanning Electron Microscope
Technic's Hummer 5 sputter-coater

Fabrication of Polymeric Membranes via a Phase Inversion Process

The compositions of membrane casting solution for the nine membranes of CP16/CP24 are shown in Table 1. Polymer components and LiCl (4-w/w%) were dissolved in 1-Methyl-2-pyrrolidone (NMP) in a clear bottle by tumbling under a heat lamp (~60°C) until forming a uniform solution.

Table 1. Composition of the CP16/CP24 membranes casting solutions.

HE1 CP24 = 0% CP16 = 12% LiBr = 4% NMP = 84%	HE4 CP24 = 0% CP16 = 14% LiBr = 4% NMP = 82%	HE7 CP24 = 0% CP16 = 18% LiBr = 4% NMP = 78%
HE2 CP24 = 6% CP16 = 6% LiBr = 4% NMP = 84%	HE5 CP24 = 7% CP16 = 7% LiBr = 4% NMP = 82%	HE8 CP24 = 9% CP16 = 9% LiBr = 4% NMP = 78%
HE3 CP24 = 12% CP16 = 0% LiBr = 4% NMP = 84%	HE6 CP24 = 14% CP16 = 0% LiBr = 4% NMP = 82%	HE9 CP24 = 14% CP16 = 0% LiBr = 4% NMP = 78%

All the membranes used in this investigation were prepared via phase inversion process. The polymeric solution was smeared on a Texlon fabric laid flat on a glass plate; the casting knife gap was set at 152 μ m (6 mils). Membrane casting speed was controlled by a D.C. motor and was set at 0.10 m/s (20 ft/min). Deionized water at 5°C was used as coagulating solution.

Membrane Pure Water Determinations

The membrane sheets were thoroughly rinsed in distilled water to remove the remaining NMP solvent in the porous membrane and 3x8 cm² (working area 22.12 cm²) coupons were used to determine the pure water flux and the "A-value" constant. Pure water permeate fluxes were measured 15 seconds after starting the cross-flow filtration operation under 275.6 Pa (40 psig) at 25°C using distilled water as feed. The A-value is expressed in units of Kg/(Pa·m²·s).

Molecular Weight Cut-Off (MWCO) Determination

Water, used for dextran solution preparation before each experiment, was purified using ion-exchange resin followed by distillation.

Dextrans of average molecular weights of 70,162, 298 and 500 kDa were employed. The dextran solution was prepared by dissolving each individual dextran in 0.10 M NaCl

solution buffered with phosphate at pH 7. The MWCO of each membrane was determined by the separation efficiency which is defined as $R=(1-C_i/C_p)$, where C_i is the concentration of the dextran present in the permeate and C_p is the concentration of the dextran in the feed. Test runs were carried out under an applied cross flow filtration pressure of 275.6 Pa at 25°C. 1.0 cc of permeate was collected at 6, 12 and 16 min after the test run was started. The Refractive Index of permeate was determined 30 min after the permeate sample was collected. The content of the Dextran in the feeds and in the permeates was determined by a “Abbe-refractometer” (0 to 10%) at 25°C by measuring the Refractive Index of the permeates and the feeds against a blank and standard solution containing 0% and 1.0% dextran, respectively. The size of the membrane coupons used was 3x8 cm² (actual membrane area 22.12 cm²). The average MWCO of the test membrane is defined as the membrane sample having a 90% or better rejection of the Dextran in the feed [14-16].

Scanning Electron Microscopy (SEM)

The cross-sectional morphologies of the membranes were sputter-coated with gold using a Technic’s Hummer 5 sputter-coated with a current of 15 mA for 3.5 min. The coated membranes were viewed with a JSM 5300 Scanning Electron Microscope, which was operated at an accelerating voltage of 10 keV.

In order to preserve the original dimensions of the pore and the porous structure of the membrane, the remaining water in the membrane was removed by a “Solvent Exchange” process which was carried out in the following manner. The wet membrane coupon was first soaked in pure isopropyl alcohol for 30 min; after that, the membrane coupon was subsequently soaked for 30 min in each isopropyl alcohol/hexane solution (75:25, 50:50 and 25:75). Finally the membrane was soaked in 100 % Hexane for 30 min. The hexane within the membrane was dried under vacuum. Sample membranes to be examined by SEM were cut out and fractured in liquid nitrogen. The dried fractured membrane samples were sputtered with gold, and then the cross-sectional scanning electron micrograph of each membrane was recorded.

Atomic Force Microscopy (AFM) of polymer membranes

The surface morphologies of the wet membranes were characterized by contact mode with a Burleigh II AFM, equipped with a non-contact/contact head and a 100 μ scanner, which was operated at a constant force mode (reference force 5nN). The wet membrane coupons were attached to a platinum sample holder that was mounted on the piezo scanner of the AFM. AFM images were acquired at a scan rate of 1.0-2.0 kHz and at an information density of 256x256 pixels (area 1μm²). The mean height is given by the average of the individual height determinations within the selected height profile.

Determination of membrane surface charge density

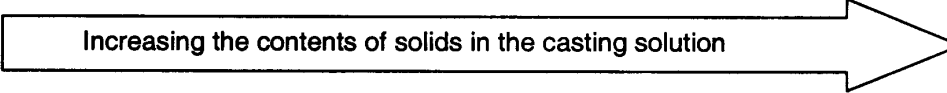
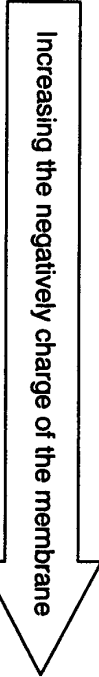
The negatively charged membranes, prepared in our laboratory, initially contain Na⁺ as the mobile counter ion. The membrane surfaces were treated with HCl (1.0 M) to replace the mobile Na⁺ counter ion by H⁺. The membranes were then rinsed with deionized water until the rinsing water reached pH 7.0. This membrane, in H⁺-form, was mounted to a special Teflon Ring having an opening area of 221.67 cm² (0.022167 m²). A measured amount of NaOH (0.010 N) solution was poured onto the membrane surface and the contact time was set at one minute. After this time the sodium hydroxide solution was poured into a beaker and titrated with dilute HCl (0.100 N) solution. The negative surface

charge density (meq/m^2) of the membrane was determined from the amount (meq) of NaOH used to neutralize the counter ion- H^+ at the membrane surface area of 221.67 cm^2 (0.022167 m^2).

Results

The experimental results indicate that the basic membrane characteristics depend on the compositions of CP16/CP24 membrane casting solutions. The trend of these changes are summarized in Table 2.

Table 2. CP-16/CP-24 membranes Characterization.

Increasing the contents of solids in the casting solution 			
Increasing the negatively charge of the membrane 	HE1 (CP16=12% CP24=0%) Thickness = 127 μm Flux velocity = 0.3519 $\text{L}/\text{m}^2\text{s}$ A* value = 1564.3×10^{-9} Water content = 85.5% 298<MWCO<500 kD Charge density = 37.458	HE4 (CP16=14% CP24=0%) Thickness = 114.3 μm Flux velocity = 0.1959 $\text{L}/\text{m}^2\text{s}$ A* value = 772.56×10^{-9} Water content = 64.9% 70<MWCO<162 kD Charge density = 47.7427	HE7 (CP16=18% CP24=0%) Thickness = 114.3 μm Flux velocity = 0.0241 $\text{L}/\text{m}^2\text{s}$ A* value = 94.31×10^{-9} Water content = 56.73% 70<MWCO<162 kD Charge density = 50.1
	HE2 (CP16=6% CP24=6%) Thickness = 106.7 μm Flux velocity = 0.26.37 $\text{L}/\text{m}^2\text{s}$ A* value = 1172.36×10^{-9} Water content = 87.4% 298<MWCO<500 kD Charge density = 42.1404	HE5 (CP16=7% CP24=7%) Thickness = 152.4 μm Flux velocity = 0.1066 $\text{L}/\text{m}^2\text{s}$ A* value = 485.69×10^{-9} Water content = 84% 162<MWCO<298 kD Charge density = 61.083	HE8 (CP16=9% CP24=9%) Thickness = 152.4 μm Flux velocity = 0.0301 $\text{L}/\text{m}^2\text{s}$ A* value = 113.8×10^{-9} Water content = 49.74% 70<MWCO<162 kD Charge density = 64.0074
	HE3 (CP16=0% CP24=12%) Thickness = 101.6 μm Flux velocity = 0.0437 $\text{L}/\text{m}^2\text{s}$ A* value = 194.14×10^{-9} Water content = 85.4% 298<MWCO<500 kD Charge density = 48.8762	HE6 (CP16=0% CP24=14%) Thickness = 177.8 μm Flux velocity = 0.0301 $\text{L}/\text{m}^2\text{s}$ A* value = 133.98×10^{-9} Water content = 54% 162<MWCO<298 kD Charge density = 65.716	HE9 (CP16=0% CP24=18%) Thickness = 165.1 μm Flux velocity = 0.0271 $\text{L}/\text{m}^2\text{s}$ A* value = 120.58×10^{-9} Water content = 45.3% 70<MWCO<162 kD Charge density = 75.5637

A-Value[=] $\text{Kg}/\text{Pa m}^2\text{s}$
Charge density [=] $\frac{\text{meq}}{\text{Lm}^2}$

For a given horizontal row of membranes, as the wt-% of the total polymer in the membrane casting solution increases, the A-value, the molecular weight cut-off (MWCO) of the membranes and the water content decrease, while the surface charge density of the membrane increases. For a given column of membranes, as the content of CP24 increases, the A-value of the membranes decrease. For membranes prepared with the highest polymer content (18 wt-%, 3th column) the surface charge density of the membrane increases as the wt-% of CP-24 (charged polymer) increases. With the exception of the membrane on the 3th column in which the water content decreases, as the wt-% of CP24 increases, the rest of the membranes on the table do not show a consistent trend on this property.

In general, the pore volume in the final coagulated membrane is controlled largely by the concentration of polymer in the casting solution. Increasing the initial polymer

concentration leads to a much higher polymer concentration at the interface. This implies that the volume fraction of polymer increases and, consequently, a lower porosity is obtained. Therefore, the pore size of the top layer can be controlled by changing the molecular weight of the polymer and polymer concentration.

As shown in Figure 2, the scanning electron micrographs (SEM) reveal that at constant total polymer solid content and for low polymer solid content membranes (HE1, HE2 and HE3) the increase of polymer CP24 wt-% in the membrane casting solution decreases the “finger print” of the cross-sectional structure of the membrane, while for high polymer content membrane (HE7, HE8 and HE9) this trend was not observed. Also for a given horizontal row of membranes, the size of the “void” and the “finger print” of the cross-sectional structure increases as the total polymer solid content increases.

We observed that the membrane surface roughness greatly depends on the composition of the membrane casting solution. As shown in the atomic force microscopy (AFM) images of this group of membranes (Figure 3), all the HE membranes exhibited similar surface morphology consisting of a rough or mottled surface with well-defined holes or shallow depressions resembling pores or channels, respectively.

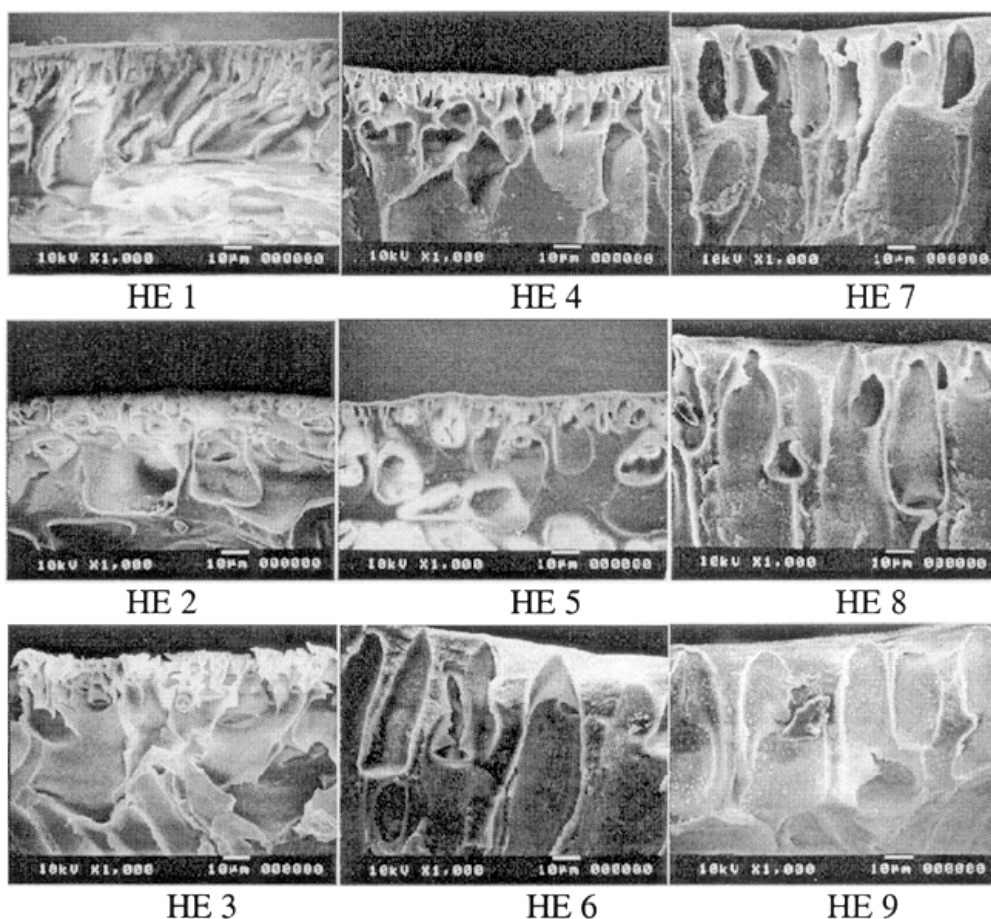


Figure 2. Scanning electron micrographs of HE series (CP16/CP24) negatively charged membranes.

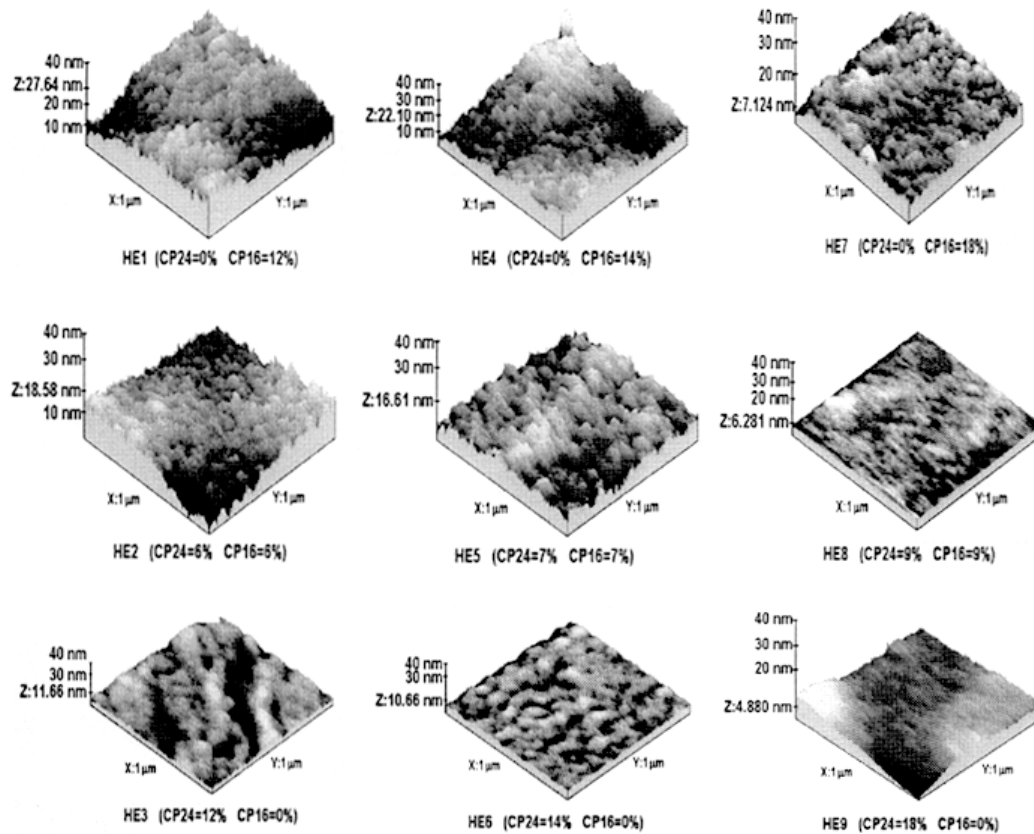


Figure 3. Atomic force micrographs of CPI6/CP24 negatively charged membranes.

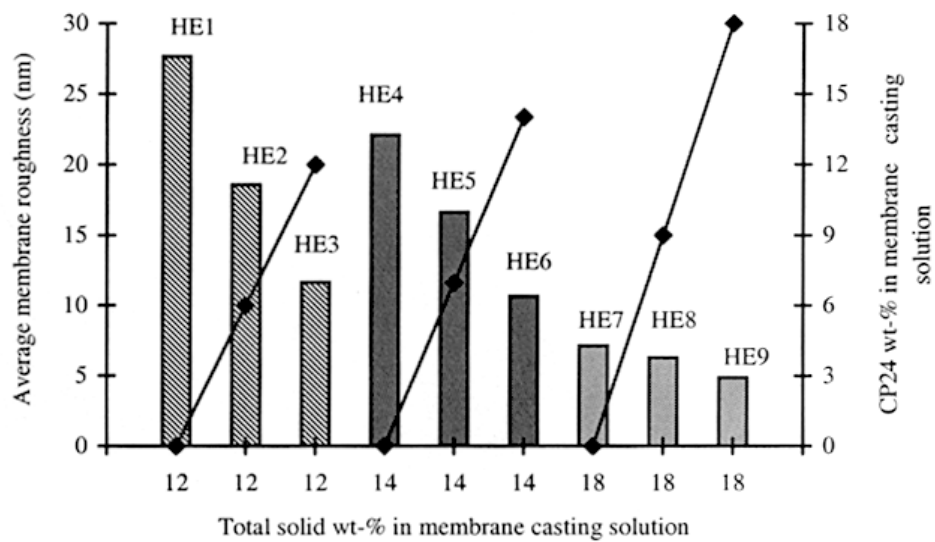


Figure 4. Dependence of average membrane surface roughness on total solid content and CP24 wt-% in membrane casting solution.

The plot of average membrane surface roughness and CP24 wt-% in membrane casting solution versus total solid wt-% in membrane casting solution (Figure 4) clearly indicates the effect of the total polymer content on the membrane surface roughness; for a given solid content, the pure CP16 membrane surface is rougher than the pure CP24 membrane surface; as the solid content in the polymer solution increases, the membrane surface becomes smoother.

Conclusions

The basic characteristics of CP16/CP24 membranes like water content, A-value, molecular weight cut-off, surface hydrophilicity, surface charge density and surface roughness can be altered by addition of the desired co-polymer in the membrane casting solutions. For most ultrafiltration applications, the membrane is required to have a smaller molecular weight cut-off with narrow pore size distribution and highly hydrophilic surface. We believe that some of our membranes prepared in this investigation may find applications in the field of wastewater treatment processes like oil-water separation that requires membranes with highly hydrophilic surfaces.

Acknowledgements: The authors thank to Dr. Miguel Parra-Hake for valuable comments on the manuscript; to Mr. Israel Gradilla M. and Dr. Leonel Cota Araiza (from CCMC-UNAM Ensenada) for performing the SEM; and to M.C. Saul Zavala and Dr. Eugenio Mendez (from CICESE Ensenada) for performing the AFM. The authors are also grateful for the support provided by CONACyT (411074-5-28023-U) and also for the Scholarship of one of the authors (HEG).

References

1. Enoch, G.D.; Van den Broche, W.F.; Spiering, W. *J Membr Sci* 1999, 87, 191.
2. Nguyen, Q.; Aotel, T.; Neel, P. *J Membr Sci* 1980, 57, 71.
3. Krehbiel, D.K.; Scamehorn, J.F.; Ritter, R.; Christian, S.D.; Tucker, E.E. *Separation Sci & Tech* 1992, 27, 1775.
4. Applegate, L.E., *Chem Eng*, 1984.
5. Han, W.; Gregor, H.P.; Pearce, E.M. *J Appl Polym Sci*, 1999, 74, 1271.
6. Knoell, T.; Safarik, K.J.; Cormack, T.; Riley, R.; Lin, S.W.; Ridgway, H. *J Membr Sci* 1999, 157, 117.
7. Düputell, D.; Staude, E. *J Membr Sci* 1993, 78, 45.
8. Cappaneelli, G.; Vigo, F.; Munari, S. *J Membr Sci*, 1983, 15, 289.
9. Kim, I.C.; Kim, J.H.; Lee, K.H.; Tal, T.M. *J Appl Polym Sci* 2000, 75, 1.
10. Kobayashi, T., Fujii, N. *J Appl Polym Sci* 1992, 45, 1897.
11. Kobayashi, T., Kumagai, K., Nosaka, Y., Miyama, H., Fujii, N., *J Appl Polym Sci* 1991, 43, 1037.
12. Tremblay, A.Y., Tam, C.M., Guiver, M.D., Dal-Cin, M.M., *J Chem Eng* 1992, 69, 1348.
13. Kim, I.C.; Choi, J.G.; Tak, T.M. *J Appl Polym Sci* 1999, 74, 2046.
14. Tremblay, A.Y., Tam, C.M., Guiver, M.D., *Ind Eng Chem Res* 1992, 31, 834.
15. Sarbolouki, M.N. *Sep Sci & Tech*, 1982, 17, 381.
16. Flegler, S.L.; Heckman, J.W.; Klopars, K.L. *Scanning and Transmission Electron Microscopy. An Introduction*. USA, 1993. Chapter 7.